Pollution Reduction and Carbon Reduction Technology Based on Pressure Swing Physical Adsorption Method in Power Enterprises

Yujia ZHANG [1]*, Gangqiang ZHANG [2]

[1] *College of Chemical Engineering, Beijing University of Chemical Technology, Beijing, 100029, China*
[2] *School of Chemical Engineering and Technology, Xinjiang University, Urumqi, Xinjiang, 830017, China*

http://doi.org/10.5755/j02.ms.38104

Received 29 July 2024; accepted 2 December 2024

With the increasing global attention to environmental issues and climate change, power companies, as an important energy production sector, are facing severe challenges in reducing pollution and carbon emissions. In view of this, this study is based on the metal organic framework MIL-101(Cr), physically encapsulating metalloporphyrins and synthesizing an iron (III) complex of tetra-p-tolylporphyrin@Materials of Institute Lavoisier-101(Cr) (FeTPP@MIL-101(Cr)) complex. Then, the surface characteristics and adsorption performance of the composite are evaluated, and the pressure swing physical adsorption method is introduced to achieve the goal of carbon reduction and pollution reduction. The ICP-OES loading results showed that the corresponding encapsulation amounts in iron (III) complex of tetra-p-tolylporphyrin@Materials of Institute Lavoisier-101(Cr)-A (MIL@-A) and iron (III) complex of tetra-p-tolylporphyrin@Materials of Institute Lavoisier-101(Cr)-B (MIL@-B) composites were 5.24 % and 3.20 %, respectively. Moreover, when the temperature increased from 273 K to 298 K, the adsorption capacity of all test gases on the three samples showed a decreasing trend. Under ideal atmospheric pressure conditions, the adsorption capacity of MIL@-A encapsulation for CO_2 did not decrease and increased, while the adsorption capacity for N_2 was relatively small, but still had a certain adsorption capacity. The above results indicate that combining the pressure swing physical adsorption method with FeTPP@MIL-101(Cr) complexes can effectively adsorb pollutants generated by power enterprises, achieve predetermined goals, and help promote clean production in power enterprises.

Keywords: electric power enterprises, pressure swing physical adsorption method, pollution reduction and carbon reduction, environmental governance, sustainable development.

1. INTRODUCTION

Global energy consumption is constantly increasing, and environmental pollution is becoming increasingly severe. The power industry, as one of the world's largest energy production and consumption industries, poses a threat to the environment and human health due to the pollutants and greenhouse gas emissions generated during the production process [1, 2]. Therefore, the development and application of effective Pollution Reduction and Carbon Reduction (PRCR) technologies are of great significance for achieving sustainable development in the power industry. Traditional PRCR technologies, such as chemical washing, Selective Catalytic Reduction (SCR), and Carbon Capture and Storage (CCS), although able to control pollutants to a certain extent, still have some limitations [3]. For example, chemical washing may generate a large amount of secondary pollutants. SCR technology has limited removal efficiency for specific pollutants, while CCS technology faces high costs and long-term storage safety issues. The increasing global emphasis on sustainable development and environmental protection has led researchers from various industries to shift their research focus toward PRCR. Deutz et al. proposed a direct air capture method based on lifecycle assessment to complete the objective of negative CEs growth. The efficiency of this method for carbon capture was higher than 85 %. Furthermore, the benefits of air capture depend on the application of energy. When using wind energy as the energy source, the impact on the environment was less than 0.057 % [4]. Sharifian and others conducted a comprehensive analysis of the flexibility and dispersion of electrochemical carbon dioxide capture technology, and found that many methods rely more on fluctuations in pH values to analyze the amount of carbon dioxide in the air. Currently, the cost of electrochemical carbon capture technology is relatively high. The application of electrodes and membranes could effectively reduce costs and facilitate the carbon economy cycle of electrification [5]. Lau et al. developed the use of Carbon Capture and Storage Technology (CCST) to decarbonize existing power plant production lines to promote the development of various power, industrial, and transportation sectors towards a low-carbon economy. They proposed a series of methods to accelerate the implementation of CCST, ultimately proving that these methods can be widely applied in the carbon treatment process of power plants [6]. Zhang's team has proposed a CCST-based emission reduction technology to reduce the near zero emission target during fossil fuel combustion. In the process, the application of CCST in hydrogen energy industrial production was investigated, and its specific application effect was analyzed. The proposed technology had a significant effect on carbon reduction, but its

* Corresponding author. Tel.: +86-17839903959; fax: +86-17839903959.
E-mail: *2021400078@buct.edu.cn* (Y. Zhang)

implementation cost was relatively high [7]. Sharma and other scholars used thermal and chemical activation methods to adsorb carbon dioxide generated during petroleum combustion, and combined metal–organic frameworks (MOFs) as a new type of adsorbent to effectively adsorb carbon dioxide. Through experimental verification, the adsorption impregnation of polyethyleneimine on solid adsorbents was the most stable [8].

Hu et al. proposed the use of the pressure swing adsorption method for the adsorption and separation of heavy products in order to improve the productivity of high-value products. After applying this method, the gas reflux rate increased by 6 % in heavy products, but decreased by 4 % in light products. In addition, this method had excellent separation performance for methane gas purity and recovery, effectively improving flow rate and enhancing product enrichment [9]. Wang's team synthesized activated carbon to enhance its Adsorption Capacity (AdC) for CO_2, and improved and explored it by integrating the properties of various composite materials. Finally, it was found that the activated carbon adsorbent has a strong AdC for CO_2 after combustion and can obtain important parameters from it [10]. Alibolandi et al. proposed a vacuum PSPAM for the separation and extraction of CO_2 generated from combustion equipment flue gas. The entire experimental process used an eight-step four-bed setup as the experimental equipment, and the experimental parameters were measured using a desktop system. It was found that when the pressure was 3.7 bar, the gas separation time was shorter [11]. Zargampoor et al. proposed an innovative vacuum oscillation and innovative mixed membrane adsorption process to remove CO_2 from flue gas. Firstly, the nanocomposite membrane adsorption system was constructed to improve the accuracy of the model, and sensitivity analysis was also conducted on the model. This method could effectively improve purity and accuracy and avoid a decrease in recovery rate [12].

Through in-depth analysis of existing literature, it is found that pressure swing physical adsorption, as a new type of environmental governance technology, has great application potential in pollutant control and carbon emission reduction due to its advantages of high efficiency, economy and simple operation. This technology can effectively remove pollutants from gases or liquids through physical adsorption, and at the same time achieve the regeneration of adsorbents under pressure swing conditions, thereby improving the recycling rate of adsorbent materials. In view of this, the study takes the metal-organic framework Material Institute Lavoisier-101 (chromium) (MIL-101 (Cr)) as the key basis, prepares a iron (III) complex of tetra-p-tolylporphyrin@Materials of Institute Lavoisier-101(Cr) ((FeTPP)@MIL-101 (Cr)) composite, and explores its performance through physical adsorption and other methods. We hope to provide power companies with an efficient, economical and environmentally friendly pollution reduction and carbon reduction technology solution and contribute to promoting the green transformation and sustainable development of the power industry.

2. MATERIALS AND METHODS

2.1. Main equipment and reagents

The preparation process of MOFs materials and their composites is usually completed in reactors and heating equipment. In the experiment, the chemical reagents used were not purified and were directly used [13, 14]. All the required solutions for the experiment were prepared using deionized water. The chemical reagents used in the experiment are all analytical grade, with a purity of over 95 %. Table 1 lists the experimental materials and reagents.

Table 1. Experimental reagents

Reagent name	Manufacturer	Reagent name	Manufacturer
1,4-terephthalic acid	Aladdin Reagent (Shanghai) Co., Ltd	Deionized water	RO reverse osmosis self-made
Nine hydrated chromium nitrate		Anhydrous ethanol	Cangzhou Dexin Biotechnology Co., Ltd
Hydrofluoric acid		Anhydrous methanol	
N. N-Dimethylformamide (DMF)		Four pairs of toluene porphyrin iron (T4MPFe, FeTPP)	Henan Weitixi Chemical Technology Co., Ltd
Sodium hydroxide		Acetone	China National Pharmaceutical Chemical Reagent Co., Ltd
Formic acid		Ammonium fluoride	McLean Reagent Co., Ltd

Except for the reagents in Table 1, the three gases used in the experiment are carbon dioxide, helium, and nitrogen, with a purity of 99.99 %. The manufacturers are all Shanxi Taineng Gas Co., Ltd. Table 2 shows the relevant equipment used in the experiment.

Table 2. Experimental equipment

Device name	Manufacturer	Type
Electronic balance	Shanghai Wujiu Automation Equipment Co., Ltd	JA2003
Ultrasonic cleaner	German company Elma	Elmasonic S
Constant temperature blast dryer	Shanghai Jiecheng Co., Ltd	DHG9240A
High speed centrifuge	Thermo Fisher	Pico 17/21
Electronic vacuum oven	Fengleng Instrument Co., Ltd	DZF-6050
Powder tablet press	Jingsheng Instrument Co., Ltd	769YP-24B
Purified water equipment	Hetai Instrument Manufacturing Co., Ltd	Eco-S15UVF
Heating Magnetic Stirrer	Meiyingpu Instrument Manufacturing Co., Ltd	MYP19-2
Ma Fulu	Thermo Fisher Scientific Co., Ltd	/
Non-stirred reactor	Century Senlang Co., Ltd	/
Rotary evaporator	Lichen Technology Co., Ltd	RE-52A

2.2. Synthesis of M–C and composite FM101C

Mix 176 mg 1.0 mmol of H_2BDC with 350 mg 1.0 mmol of metal salt chromium nitrate nine water, stir thoroughly and mix well before adding 5 mL of deionized water solution. After thoroughly stirring again, add 0.05 ml of 35 % HF solution to the mixture [15]. Load the mixture into the reactor and heat it at 220 ℃ for about 8 hours to obtain the required M-C substance for the experiment, which appears as a gray-green crystalline substance. Subsequently, the crystals are cleaned, dried, and ground into powder for use. Adopting composite packaging technology for FM101C composite material for preparation. Fig. 1 shows the operation process.

Fig. 1. Synthesis of MIL complex

Based on the powder prepared in Fig. 1, this study added cleaning and purification steps. This is similar to the MOF synthesis process, but the difference lies in the introduction of porphyrin ring macromolecules. In sample bottle 1, dissolve 10 mg or 20 mg of porphyrin macromolecules in a 2.5 ml deionized aqueous solution containing 350 mg of chromium nitrate nine hydrate. Continue stirring for 5 minutes to ensure uniform mixing, then add 176 mg of H_2BDC in an acidic environment. Pour the contents obtained from two sample bottles into a reaction vessel lined with polytetrafluoroethylene and continue stirring for about 8 minutes. Seal and heat in a high-temperature oven at 220 ℃ for 8 h. After filtering, obtain the desired dark green crystals. After cleaning and purification, dry the solid product in a vacuum drying oven at 75 ℃ for 10 h. According to the different amounts of porphyrin molecules added (10 mg and 20 mg respectively), the resulting composite materials are named as FeTPP@ML-101(Cr)-A and FeTPP@ML-101(Cr)-B.

2.3. Cleaning and purification of MOFs and complexes

M–C has received widespread attention from industry scholars due to its wide range of applications and strong adaptability [16]. However, during the synthesis process, due to the low-solubility of terephthalic acid in water, the newly synthesized M–C crystal may contain a significant amount of unreacted terephthalic acid. This will clog the pores of the material, causing its specific surface area (SSA) and pore volume to be lower than the theoretical values, thereby affecting its practical application [17]. To obtain pure crystals, it is usually needed to utilize hot solutions like ethanol or ammonium fluoride to purify the crystal material.

To purify the large number of unreacted white needle-like ligands that may be blocked in the pores of the synthesized sample, the experiment proposes to use cold washing solutions (anhydrous methanol, acetone, DMF) for sequential cleaning. Acetone and DMF are mainly used to remove unreacted organic ligands, while anhydrous methanol is used as a universal cleaning agent [18]. After cleaning, rinse the sample thoroughly with deionized water. Next, perform a hot washing treatment using anhydrous ethanol and ammonium fluoride solution. Add 10 ml of anhydrous ethanol to the sample after cold washing, and then heat the sample bottle in an oil bath at 100 ℃ for 20 h. After filtration, remove the purified sample and wash it with pure water to remove residual ethanol. Finally, add 10 mL of 1 M ammonium fluoride solution and heat the sample in a 70 ℃ oven for 1 d. After removing the sample, filter and dry it to obtain the desired pure crystal.

2.4. Material characterization and adsorption performance testing

To detect the raw materials and the prepared composites, X-ray diffraction (XRD), Fourier transform infrared spectroscopy (FTIR), SSA and pore size testing, thermogravimetric analysis (TGA), scanning electron microscopy (SEM) crystal phase analysis, inductively coupled plasma (ICP) spectroscopy, and pure component gas static adsorption testing are used for performance analysis in the experiment.

XRD: XRD analysis was carried out using a Rigaku SmartLab XRD instrument equipped with a Cu K_α radiation source (λ = 1.5406 Å). The operational parameters were set at a voltage of 40 kV and a current of 30 mA. The scanning was performed in the 2θ range of 5° to 80° with a step size of 0.02° and a scan speed of 1°/min. This device provided high-resolution data to ensure precise phase identification and analysis of the crystallographic properties of the synthesized composites. The samples for XRD analysis were prepared by grinding the synthesized composites into a fine powder using a mortar and pestle. The powdered samples were mounted onto glass slides with the aid of adhesive to ensure even distribution and minimize sample displacement. To enhance the analysis accuracy, the samples were activated at 150 °C under vacuum conditions for 6 hours prior to characterization, ensuring the removal of any adsorbed moisture or solvents from the pores.

FTIR: completed on Thermo Scientific Nicolet iS50., tested in the wave number range of 400 – 2000 cm^{-1}.

SSA and pore size test: N_2 adsorption-desorption curve and pore size distribution test were measured on Micromertics ASAP 2460 physical adsorption instrument. Before the test, the sample needs to be activated for 6 h in a vacuum environment at 150 ℃.

TGA: TGA was carried out on STA409 thermogravimetric (TG) analyzer., tested in N_2 atmosphere, with a test temperature range of 30 ~ 900 ℃ and a heating rate of 5 ℃/min.

SEM crystal phase analysis: SEM electron microscopy characterization was tested on a Zeiss EvoLS 15 electron microscope, with a test voltage of 3 kV.

ICP: The concentrations of various components in the samples were measured using an inductively coupled plasma optical emission spectrometer (ICP-OES, Perkin Elmer Avio 200), operating in axial plasma view mode with an ultrasonic nebulizer and a charge-coupled detector.

3. RESULTS AND DISCUSSION

3.1. XRD and FTIR

To analyze the intrinsic structure, appearance, and encapsulation effect of FeTPP packaged samples, this study conducts XRD analysis on the prepared samples, as displayed in Fig. 2 a. The diffraction peaks of the newly synthesized FM101C and M–C are the same. This indicates that encapsulating FeTPP does not alter the M-C's structural integrity. However, the main peak value of the sample significantly increases after packaging, which may be due to the material adhering to the surface and related to internal filling and grain growth. To confirm whether the FeTPP sample has been successfully encapsulated in the pores of M–C, FTIR analysis is performed on the sample in this study, as exhibited in Fig. 2 b.

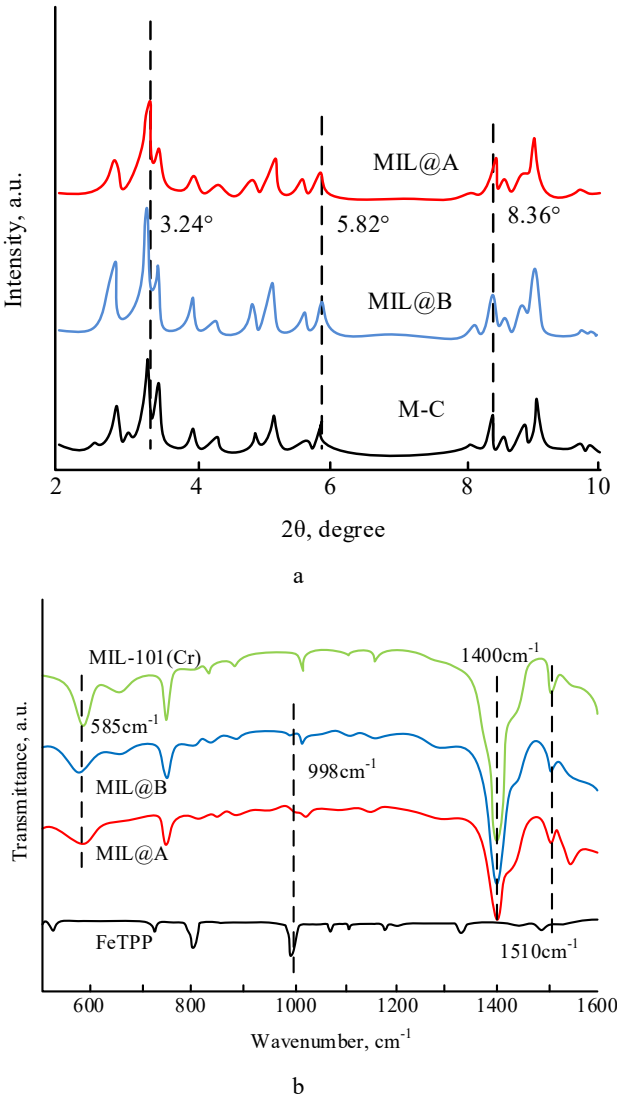

Fig. 2. a – XRD patterns; b – FTIR spectra

The vibration distribution of the main chemical groups and bonds ranges from 500 to 1600 cm^{-1}. In addition to the common skeletal characteristic peaks of the complex and the original MOF, such as the antisymmetric and symmetric stretching vibration peaks of benzoic acid (1510, 1400 cm^{-1}) and the Cr–O (585 cm^{-1}), a unique pyrrole ring peak (998 cm^{-1}) of metalloporphyrin macromolecules is also observed in the spectrum of FM101C. The appearance of this characteristic peak is partly attributed to the stretching vibration mode of the C–C bond and the phenyl C=C bond in the pyrrole ring, thereby confirming the existence of FeTPP in FeTPP@MIL-101 (Cr) and the successful encapsulation of porphyrin molecules in the complex. XRD analysis and FTIR analysis were conducted at room temperature of 25 ℃.

3.2. Brunauer-Emmett-Teller (BET) specific surface area test

The nitrogen adsorption-desorption isotherm is a technique utilized to characterize the pore structure of materials, and the curve changes of this isotherm directly reflect the characteristics of the internal pore structure of materials. The adsorption-desorption curve and pore size distribution (PSD) are tested using the Micromeritics ASAP 2460 physical adsorption analyzer. Under the condition of 77 K, nitrogen is used for adsorption and desorption experiments. Before testing, the sample is required to be activated in a vacuum environment at 150 °C for 6 h to ensure the accuracy of the test results. The results obtained are shown in Fig. 3.

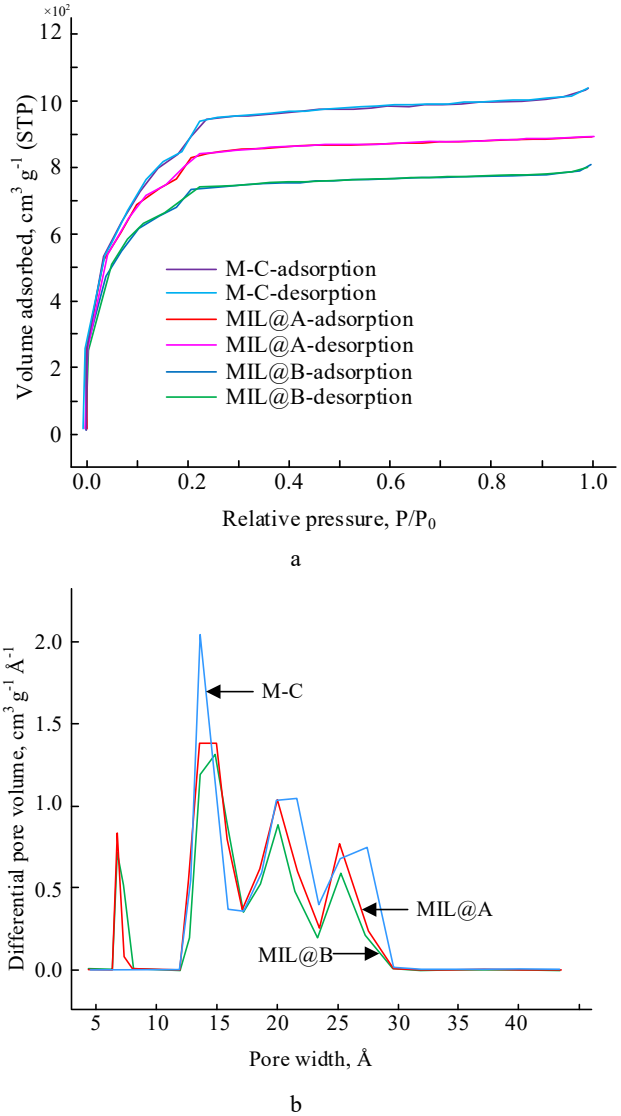

Fig. 3. BET specific surface area test results: a – nitrogen adsorption-desorption isotherm at 77 K; b – PSD of M-C and the prepared composite material

Fig. 3 a shows the variation of nitrogen adsorption-desorption isotherms at 77 K. All curves exhibit Type I isotherms, indicating that the material mainly contains microporous structures. In addition, a certain proportion of mesopores are detected in the material, and the pore structure of the material is semblable to that of the original MOF. Fig. 3 b shows the PSD of M–C and the prepared composite material. The data shows that the pore size of M–C is mainly concentrated around 1.3 nm, 1.7 nm, and the mesopores around 2.0 nm and 2.3 nm, which are like the pore size of the original MOF. However, with the increase in load, additional micropores of about 0.7 nm appear in the material, and the number of micropores increases. Although this is beneficial for the adsorption of specific gases, excessive encapsulation may lead to more space being filled, thereby reducing pore volume. Table 3 shows the specific SSA and PSD for various samples.

Table 3. Results of SSA and PSD of different samples

Sample name	S_{BET}, m^2/g	Slangmuir, m^2/g	V_{total}, cm^3/g	V_{mic}, cm^3/g	V_{mic}/V_{mes}, %
M-C	3001.8	4541.3	1.701	1.357	79.8
MIL@-A	2889.9	3874.6	1.412	1.209	85.6
MIL@-B	2657.3	3507.4	1.191	1.074	90.2

In Table 3, compared to M–C, the BET SSA of the prepared composite FeTPP decreases from 3001.8 m^2/g to 2889.9 m^2/g and 2657.3 m^2/g, respectively. Meanwhile, the pore size shows a significant decrease. This is consistent with the results obtained in Fig. 3, where the PSD and SSA of the original MOF and composite materials are very similar.

3.3. TGA

TG is a thermal analysis method that monitors sample quality changes with temperature under programmed temperature control, commonly used to evaluate the thermal stability and composition of materials. The sample used in this study is approximately 15 mg and tested in a nitrogen environment. The nitrogen flow rate is set to 30 mL/minute. The temperature range for testing is from 30 °C to 900 °C, with a heating rate of 5 °C per minute. Additionally, TGA is performed using the STA409 TG analyzer in a nitrogen atmosphere. The testing temperature is set to 35 °C to 600 °C, and the heating rate is also 5 °C per minute. The results of using TG technology to investigate the thermal stability of FeTPP encapsulated materials and determine the optimal activation temperature of the adsorbent are shown in Fig. 4.

In Fig. 4, the loss curve of the obtained composite is very similar to M–C and contains two stages. Stage 1 is between 30 °C and 300 °C, and the weight reduction is mainly due to the evaporation of solvent molecules, such as water, methanol, and DMF. When the temperature rises to around 350 °C, weight loss begins to occur. This indicates that as the temperature further increases, the structure of the material begins to disintegrate and begin to decompose. Therefore, before officially starting the adsorption test, the material must be activated at 150 °C for 6 h to ensure that solvent molecules in the adsorbent pores are completely eliminated.

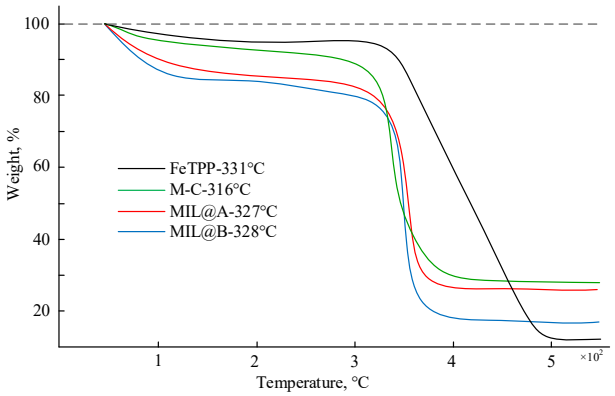

Fig. 4. TG curve results

3.4. SEM crystal phase analysis

SEM is mainly taken to observe the microstructure of materials, the size of crystal particles, and their degree of crystallization. The sample is first uniformly dispersed in an ethanol solution, and then dropped onto an aluminum foil coated with conductive adhesive. After vacuum coating, the sample surface is coated with a gold layer to improve its conductivity, and then observed by SEM. The characterization test of SEM is conducted on the Zeiss EvoLS 15 electron microscope, using a voltage of 3 kV during the test. Fig. 5 shows the obtained SEM image.

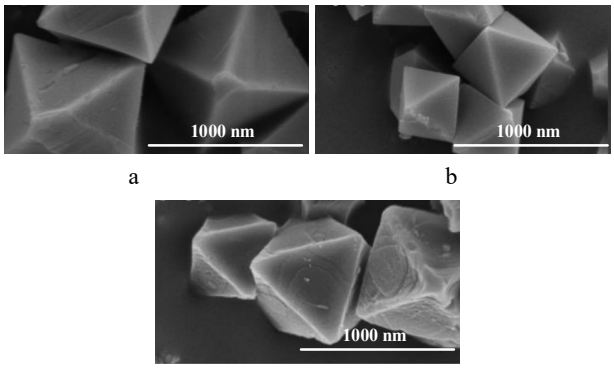

Fig. 5. SEM image of sample: a – image of MIL-101(Cr); b – image of MIL@A; c – image of MIL@B

In Fig. 5, there is no obvious change in the structure and shape of the sample B&A packaging, and the morphology of the prepared composite still exhibits a regular octahedral shape. However, the surface of the packaged sample is not as smooth and regular as the original material, and this change may be due to the accumulation of internal pores during the synthesis process and the adhesion of the material surface to the wall.

3.5. ICP-OES load analysis

To determine the content of FeTPP in the prepared samples, ICP-OES analysis was performed on the synthesized samples. Fig. 4 shows the result of diluting the sample with hydrochloric acid aqueous solution before testing. In Table 4, the Cr content and Fe content in MIL@-A and MIL@-B composites account for 16.78 % and

0.32 %, and 15.02 % and 0.47 %, respectively. At this point, the corresponding FeTPP packaging amounts are 5.24 % and 3.20 %

Table 4. ICP-OES load test

Complex	Cr content, %	Fe content, %	Packaging quantity, %
MIL@-A	16.78	0.32	5.24
MIL@-B	15.02	0.47	3.20

3.6. Static adsorption testing and adsorption heat analysis of pure component gases

To verify the effectiveness of the packaging strategy adopted and investigate the effect of FeTPP packaging on the adsorption performance of M–C, this study tested the adsorption isotherms of CO_2 and N_2 pure components of M–C and its composites under 273 K and 298 K conditions. Through experiments, the changes in CO_2 and N_2 isothermal AdC of the original MOF and its composites can be obtained at specific temperatures. Further investigation reveals key performance indicators such as material separation selectivity and adsorption heat, as shown in Fig. 6.

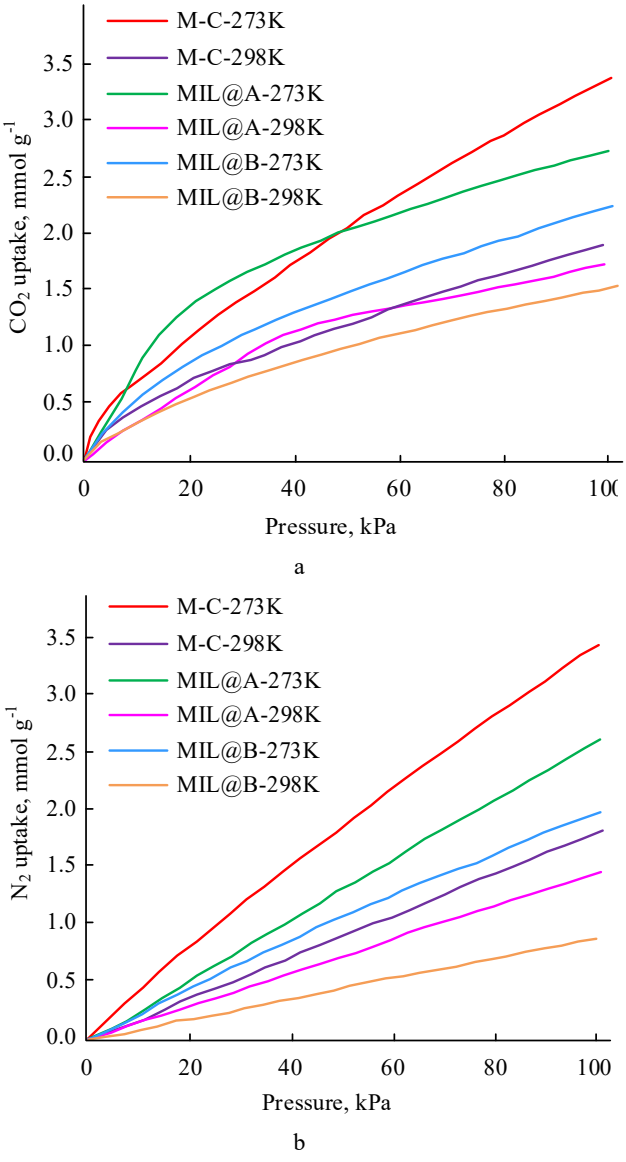

Fig. 6. Isothermal adsorption curve: a – CO_2 uptake; b – N_2 uptake

Fig. 6 shows the isothermal adsorption curves of carbon dioxide and nitrogen for different materials, respectively. As the temperature increases from 273 K to 298 K, the AdC of all test gases on the 3 samples shows a decreasing tendency. This indicates that the entire adsorption process is mainly physical adsorption. Physical adsorption can usually occur on any solid surface, and the adsorption process is directly affected by the SSA. When the temperature and pressure of the reaction are different, the addition of porphyrin reduces the SSA and pore volume of the composite FeTPP, thereby reducing its absorption of N_2 in contrast with the original M-C. When the pressure is the same, the AdC of CO_2 by M-C and FM101C exceeds that of N_2, indicating a better interaction between CO_2 and the adsorbent. With the increase of FeTPP encapsulation amount and the continuous increase of reaction temperature, the equilibrium AdC of N_2 begins to decrease continuously, and under normal pressure, the AdC of CO_2 also shows a similar trend. In Fig. 6 a, under low pressure conditions, especially below 40 kPa, the FM101C composite material significantly enhances its CO_2 absorption capacity. This is mainly due to the increase in microporous structures in the material, which provides more adsorption sites for CO_2 molecules under low pressure conditions. However, at room temperature of 298 K and high loading capacity (20 mg), the increase in related AdC is not significant due to the possibility of pore blockage. With the increase of pressure, even at room temperature, an appropriate amount of loading can make the absorption of CO_2 exceed the original MOF structure, and the manifestation of the microporous effect may be slightly delayed. In Fig. 6 b, in the adsorption between the material and N_2, the adsorption amount shows a decreasing trend with the increase of encapsulation amount. The addition of an appropriate amount of FeTPP provides more adsorption sites for CO_2 molecules, thereby enhancing the interaction with FM101C molecules. However, excessive FeTPP loading does not continuously enhance this interaction and may instead lead to a decrease in adsorption performance. This emphasizes the necessity of controlling the packaging amount reasonably in the preparation process of composite materials. In addition, the strong adsorption and high polarization between CO_2 molecules and FM101C can be further verified by measuring an equal amount of adsorption heat. In summary, compared with the adsorption of N_2, under the same experimental conditions, FM101C has a better adsorption effect on CO_2. This phenomenon can be explained as CO_2 molecules having smaller motion diameters and higher polarizability. This makes them encounter fewer obstacles during the diffusion process, making it easier to penetrate and fill into the microporous space composed of M–C and FeTPP. To deeply analyze the effect of FeTPP encapsulation on the performance of adsorbents, this study compares the changes in isothermal adsorption heat under two different temperature conditions, as shown in Fig. 7. In Fig. 7, FM101C exhibits significantly higher adsorption heat for CO_2 at atmospheric pressure than M–C. This phenomenon reveals that the addition of FeTPP significantly improves the AdC for CO_2. This enhanced adsorption can be explained by the synergistic effect between Cr(II) open metal sites and Fe-based porphyrin rings. CO_2 molecules tend to aggregate in the microporous space composed of M-C and FeTPP. However, increasing

the loading amount of FeTPP does not further enhance the AdC for CO_2, but rather may lead to a decrease in AdC due to the reduction of SSA and PSD.

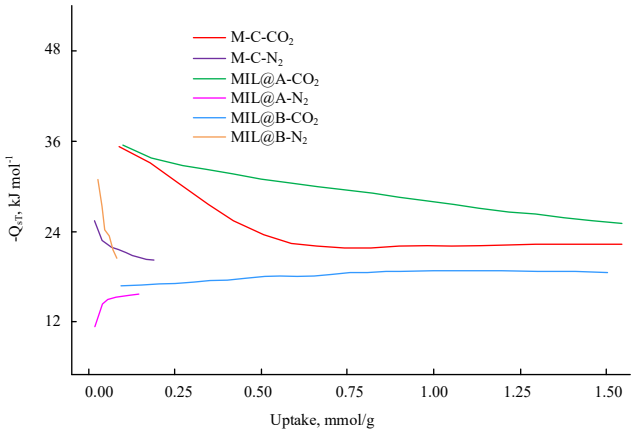

Fig. 7. Comparison of isotope adsorption heat

Among the three samples, except for MIL@-B, the equal adsorption heat Q_{st} of CO_2 is generally higher than that of N_2, indicating that CO_2 has a stronger adsorption force and higher adsorption rate during the adsorption process. This gives CO_2 a certain advantage in the adsorption competition with other gases. For MIL@-A, the adsorption heat of N_2 has decreased. This may be due to the greater influence of inner wall and pore volume on N_2 adsorption, while specific metal ions have less support for N_2 adsorption. In addition, excessive additive molecules may hinder the interaction between N_2 and the adsorbent. For MIL@-B, although it provides more adsorption sites, it does not enhance its AdC for CO_2, but rather reduces its selectivity. The equivalent adsorption heat of N_2 in MIL@-A ranges from 12.0 to 16.0 kJ/mol, which is relatively low. This may be related to the "sieve effect" generated by the gaps, which hinders the AdC of N_2 molecules with larger motion diameters.

3.7. Adsorption selectivity of FM101C

The analysis of the AdC and phase changes of different substances on each component after mixing two gases is shown in Fig. 8. In Figure 8, the ratio of CO_2 to N_2 is 3:17. In mixed gases, the adsorption behavior of N_2 is like the adsorption mode of a single gas. However, the adsorption behavior of CO_2 is significantly different. Under normal pressure conditions, especially under MIL@-A packaging conditions, the adsorption of CO_2 does not decrease, but rather increases. This indicates that, under appropriate pore structure and volume, an appropriate amount of FeTPP can provide more adsorption sites for CO_2 and FM101C. However, excessive packaging can weaken the adsorption effect, and whether it is a single gas or a mixed gas, the AdC will decrease under normal pressure. This is because excessive encapsulation material can accumulate on pores and adsorption surfaces, hindering the adsorption process. Meanwhile, the AdC of N_2 in the mixed gas follows a decreasing trend of the AdC of a single component of nitrogen. As the packaging amount increases, the SSA decreases, leading to a decrease in equilibrium AdC. This difference is a key factor leading to the selective adsorption of CO_2/N_2.

3.8. Discussion

To actively respond to the challenges of pollution reduction and carbon reduction in the whole society, the experiment proposed a method of using the metal-organic framework MIL-101 (Cr) as the basis and adding metal porphyrin as an encapsulant to produce FeTPP@MIL-101 (Cr) composites.

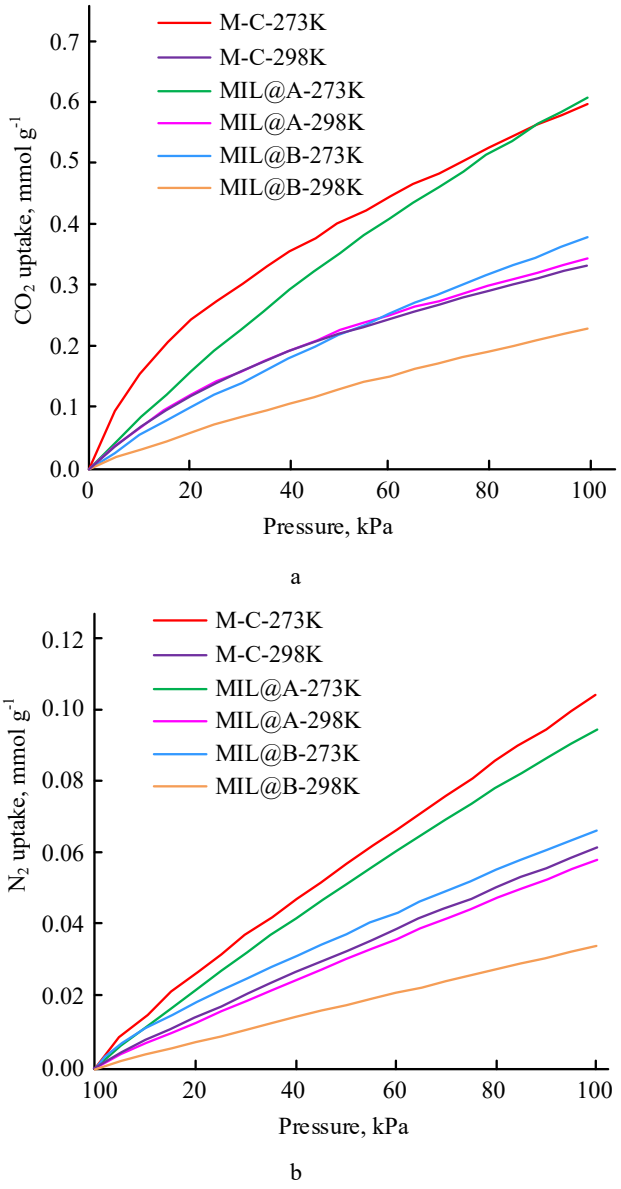

Fig. 8. AdC of different substances on CO_2 and nitrogen components: a – adsorption amount of each CO_2 component; b – adsorption amount of each component of N_2

The results showed that under low pressure conditions, the adsorption amount of the composite for all test gases showed a downward trend, indicating that the entire adsorption process was mainly physical adsorption. At the same time, with the increase in encapsulation amount, the adsorption amount showed a downward trend. The addition of an appropriate amount of FeTPP provides more adsorption sites for CO_2 molecules, thereby enhancing the interaction with FeTPP@MIL-101 (Cr) molecules. Zhu and other scholars believe that amine-containing porous

materials have a large carbon dioxide adsorption capacity and good stability [19]. This is consistent with the findings of the study. Although the adsorption amount decreased under the condition of increasing the encapsulation amount, the performance of the composite has been very stable. Hense et al. proposed to adjust the pressure through a dynamic simulation model to adsorb greenhouse gases, and the use of renewable energy can further adsorb greenhouse gases, ultimately providing a feasible short-term solution for the adsorption of greenhouse gases [20]. The study found that under normal pressure conditions, especially under MIL@A packaging conditions, the adsorption of CO_2 increased significantly; and the adsorption of N_2 in the mixed gas followed the downward trend of the adsorption of single component nitrogen. This is highly consistent with the research results of Hense et al., and the change in pressure has a significant effect on the adsorption of greenhouse gases. However, since the selection of materials has a significant impact on the results, the price of the selected materials must be considered in practical applications. Therefore, subsequent experiments need to further explore the use of affordable consumables to carry out experiments.

3. CONCLUSIONS

With the development of industrialization, global climate change and environmental pollution are becoming increasingly serious, posing a serious threat to human society and the ecosystem. In particular, the increasing greenhouse gas emissions from the power industry have not only led to global warming, but also had a profound impact on climate patterns. In this context, the experiment was based on FeTPP@MIL-101(Cr) composite, and different amounts of porphyrin were added to explore the adsorption performance of the encapsulated FeTPP composite on greenhouse gases. The research results show that:

1. When the pressures are the same, the adsorption capacity of CO_2 by the raw material MIL-101(Cr) and the prepared FeTPP@MIL-101(Cr) composite far exceeds that of N_2.
2. Especially under low pressure conditions, the CO_2 absorption capacity of the composite FeTPP@MIL-101(Cr) increases significantly.
3. In addition, the adsorption heat of CO_2 of FeTPP@MIL-101(Cr) under normal pressure is significantly higher than that of MIL-101(Cr). The above results all show that by changing the pressure value, the adsorption performance of the prepared composite for greenhouse gases can be effectively improved and energy consumption can be reduced.

REFERENCES

1. **Erans, M., Sanz-Pérez, E.S., Hanak, D.P., Clulow, Z., Reiner, D.M., Mutch, G.A.** Direct Air Capture: Process Technology, Techno-economic and Socio-political Challenges *Energy & Environmental Science* 15 (4) 2022: pp. 1360 – 1405. https://doi.org/10.1039/d1ee03523a
2. **Lai, J.Y., Ngu, L.H., Hashim, S.S.** A Review of CO_2 Adsorbents Performance for Different Carbon Capture Technology Processes Conditions *Greenhouse Gases: Science and Technology* 11 (5) 2021: pp. 1076 – 1117. https://doi.org/10.1002/ghg.2112
3. **Ramar, V., Balraj, A.** Critical Review on Carbon-based Nanomaterial for Carbon Capture: Technical Challenges, Opportunities, and Future Perspectives *Energy & Fuels* 36 (22) 2022: pp. 13479 – 13505. https://doi.org/10.1021/acs.energyfuels.2c02585
4. **Deutz, S., Bardow, A.** Life-cycle Assessment of an Industrial Direct Air Capture Process Based on Temperature–vacuum Swing Adsorption *Nature Energy* 6 (2) 2021: pp. 203 – 213. https://doi.org/10.1038/s41560-020-00771-9
5. **Sharifian, R., Wagterveld, R.M., Digdaya, I.A., Xiang, C.X., Vermaas, D.A.** Electrochemical Carbon Dioxide Capture to Close the Carbon Cycle *Energy & Environmental Science* 14 (2) 2021: pp. 781 – 814. https://doi.org/10.1039/d0ee03382k
6. **Lau, H.C., Ramakrishna, S., Zhang, K., Radhamani, A.V.** The Role of Carbon Capture and Storage in the Energy Transition *Energy & Fuels* 35 (9) 2021: pp. 7364 – 7386. https://doi.org/10.1021/acs.energyfuels.1c00032
7. **Zhang, L., Sun, N., Wang, M., Wu, T., Wei, W., Pang, C.H.** The Integration of Hydrogenation and Carbon Capture Utilisation and Storage Technology: A Potential Low - carbon Approach to Chemical Synthesis in China *International Journal of Energy Research* 45 (14) 2021: pp. 19789 – 19818. https://doi.org/10.1002/er.7076
8. **Sharma, H., Dhir, A.** Capture of Carbon Dioxide Using Solid Carbonaceous and Non-carbonaceous Adsorbents: a Review *Environmental Chemistry Letters* 19 (2) 2021: pp. 851 – 873. https://doi.org/10.1007/s10311-020-01118-2
9. **Hu, G., Guo, Y., Zhao, Q., Xiao, G., Li, K.G., May, E.F.** Separation of Methane and Nitrogen Using Heavy Reflux Pressure Swing Adsorption: Experiments and Modeling *Industrial & Engineering Chemistry Research* 62 (18) 2023: pp. 7114 – 7126. https://doi.org/10.1021/acs.iecr.3c00094
10. **Wang, J., Pu, Q., Ning, P., Lu, S.** Activated Carbon - based Composites for Capturing CO_2: a Review *Greenhouse Gases: Science and Technology* 11 (2) 2021: pp. 377 – 393. https://doi.org/10.1002/ghg.2051
11. **Alibolandi, M., Sadrameli, S.M., Rezaee, F., Darian, J.T.** Separation of CO_2/N_2 Mixture by Vacuum Pressure Swing Adsorption (VPSA) Using Zeolite 13X Type and Carbon Molecular Sieve Adsorbents *Heat and Mass Transfer* 56 (6) 2020: pp. 1985 – 1994. https://doi.org/10.1007/s00231-020-02823-y
12. **Zarghampoor, M.H., Soleimani, M., Mozaffarian, M., Ravanchi, M.T.** New Hybrid Membrane Vacuum Swing Adsorption Process for CO_2 Removal from N_2/CO_2 Mixture: Modeling and Optimization by Genetic Algorithm *Environmental Science and Pollution Research* 29 (60) 2022: pp. 90820 – 90834. https://doi.org/10.1007/s11356-022-22080-2
13. **Joel, A.S., Isa, Y.M.** Novelty in Fossil Fuel Carbon Abatement Technologies in the 21st Century: Post - Combustion Carbon Capture *Journal of Chemical Technology & Biotechnology* 98 (4) 2023: pp. 838 – 855. https://doi.org/10.1002/jctb.7281

14. **Talei, S., Soleimani, Z.** Comparative Analysis of Three Different Negative Emission Technologies, BECCS, Absorption and Adsorption of Atmospheric CO *Civil and Environmental Engineering Reports* 31 (3) 2021: pp. 99 – 117.
https://doi.org/10.2478/ceer-2021-0036

15. **Kumar, R., Mangalapuri, R., Ahmadi, M.H., Vo, D.V.N., Solanki, R., Kumar, P.** The Role of Nanotechnology on Post-combustion CO_2 Absorption in Process Industries *International Journal of Low-Carbon Technologies* 15 (3) 2020: pp. 361 – 367.
https://doi.org/10.1093/ijlct/ctaa002

16. **Chari, S., Sebastiani, A., Paulillo, A., Materazzi, M.** The Environmental Performance of Mixed Plastic Waste Gasification with Carbon Capture and Storage to Produce Hydrogen in the UK *ACS Sustainable Chemistry & Engineering* 11 (8) 2023: pp. 3248 – 3259.
https://doi.org/10.1021/acssuschemeng.2c05978

17. **Kazemifar, F.** A Review of Technologies for Carbon Capture, Sequestration, and Utilization: Cost, Capacity, and Technology Readiness *Greenhouse Gases: Science and Technology* 12 (1) 2022: pp. 200 – 230.
https://doi.org/10.1002/ghg.2131

18. **Fahr, S., Powell, J., Favero, A., Giarrusso, A.J., Lively, R.P., Realff, M.J.** Assessing the Physical Potential Capacity of Direct Air Capture with Integrated Supply of Low-carbon Energy Sources *Greenhouse Gases: Science and Technology* 12 (1) 2022: pp. 170 – 188.
https://doi.org/10.1002/ghg.2136

19. **Zhu, X.C., Xie, W.W., Wu, J.Y., Miao, Y.H., Xiang, C.J., Chen, C.P., Ge, B.Y., Gan, Z.Z., Yang, F., Zhang, M., O'Hare, D., Li, J., Ge, T.S., Wang, R.Z.** Recent Advances in Direct Air Capture by Adsorption *Chemical Society Reviews* 51 (15) 2022: pp. 6574 – 6651.
https://doi.org/10.1039/d1cs00970b

20. **Hense, J., Bachmann, M., Polte, L., von der Aßen, N., Jupke, A.** Integrated Process Design and Life Cycle Assessment of Carbon Monoxide Provision from Basic Oxygen Furnace Gas *Chemie Ingenieur Technik* 94 (10) 2022: pp. 1524 – 1535.
https://doi.org/10.1002/cite.202200029